

Date of publication xxxx 00, 0000, date of current version xxxx 00, 0000.

Digital Object Identifier 10.1109/ACCESS.2022.Doi Number

# Compact reconfigurable MIMO antenna for 5G and Wi-Fi applications

Widad A Mshwat <sup>1</sup>, Jamal Kosha <sup>1</sup>, Abubakar Salisu <sup>1</sup>, Atta Ullah <sup>1</sup>, Nazar T. Ali <sup>2</sup>, Issa, Elfergani <sup>1,3</sup>, Chan Hwang See <sup>4</sup>, Chemseddine Zebiri <sup>5</sup>, Jonathan Rodriguez <sup>3</sup>, Raed Abd-Alhameed <sup>1,6\*</sup>

<sup>1</sup>Faculty of Engineering and Digital Technologies, University of Bradford, Bradford BD7 1DP, UK

<sup>2</sup>Khalifa University, United Arab Emirates

<sup>3</sup>Mobile Systems Group, Instituto de Telecomunicações, 3810-193 Aveiro, Portugal;

<sup>4</sup>School of Computing, Engineering and the Built Environment, Edinburgh Napier University, Edinburgh EH10 5DT, U.K

<sup>5</sup>Department of Electronics, University of Ferhat Abbas, Setif -1-, 19000 Setif, Algeria;

<sup>6</sup>Department of Communication and Informatics Engineering, Basra University of Science and Technology, Basrah, 61004 Iraq

Corresponding author: [r.a.a.abd@bradford.ac.uk](mailto:r.a.a.abd@bradford.ac.uk)

**ABSTRACT** Four miniaturized four-element multiple-input multiple-output (MIMO) antenna designs are proposed, designed, and fabricated with dimensions of 26 mm x 26 mm x 0.8 mm each. The first MIMO design operates at 3.5 GHz, while the second operates at 5.2 GHz. The first and second designs are combined into a third design that can be reconfigured to operate at either 3.5 GHz or 5.2 GHz. A new concept of balance is introduced to address the issue of small ground faced by the previous designs. This concept is applied to the third antenna design, resulting in a fourth design of reconfigurable MIMO operating at 5.2 GHz or 3.5 GHz. The antenna demonstrates good impedance matching at both operating frequencies, with isolation levels of approximately 25 dB and 21 dB, envelope correlation coefficients (ECC) less than 0.0001, diversity gain (DG) of around 10 dB at both frequencies, and peak realized gains of 3.5 dBi at 3.5 GHz and 4 dBi at 5.2 GHz. The radiation efficiency of the fourth compact antenna design is approximately 88% at 3.5 GHz and 91% at 5.2 GHz. The measured results show excellent agreement with the simulated results for all four antenna designs.

**INDEX TERMS** Frequency reconfigurable MIMO antenna; PIN diode; isolation; envelope correlation coefficient (ECC)

## I. INTRODUCTION

With the continuous-increasing congestion of the EM spectrum and growing bandwidth demand, reconfigurable antennas have acquired a lot of attention because of their ability to change the band of their operating frequency based upon the availability of spectrum and hence, customize themselves to the needs of a dynamic environment, thereby increasing the frequency spectrum utilization efficiency. Furthermore, frequency reconfigurable antennas are suitable for a wide range of future wireless communication applications due to their small size, easy integration, low cost, wideband or narrow band operation, single-band or multi-band configurations, and frequency selectivity ability to decrease jamming and co-site interference [1-3]. Switches in radiating components or microstrip feedlines can be used to achieve frequency reconfigurability.

In frequency reconfigurable antennas and MIMO antennas, the usage of the reconfigurable feedline is critical for achieving diversity and producing varied radiation characteristics. Furthermore, reconfigurable feedlines facilitate reconfigurability without the need to include active

components on the antenna's radiating structure, which decreases losses, saves costs, and reduces undesired radiation interference on mounted antennas caused by biasing lines [4]. For contemporary communication systems, frequency reconfigurable antennas utilising tuneable feedlines are particularly desired.

Patch antennas are appealing options for frequency reconfigurable antenna designs because of their planar structure and low profile, low cost, lightweight, ease of production, and ease of integration with various electrical components and devices. [5-14] have described a variety of frequency reconfigurable patch antennas that operate in the 1.5–13 GHz frequency region. PIN diodes [5-8], Varactor diodes [9-13], or MEMS (microelectromechanical systems) switches [14] were included in the radiating structure to provide frequency reconfigurability in these antenna designs. Two frequency reconfigurable patch antennas were presented in [5] and [6], which can change resonant frequencies between 3.5GHz and 1.7GHz. Patch elements of 18x 29mm<sup>2</sup> were used in these designs. A frequency and pattern reconfigurable patch antenna capable of operating at

3.3GHz and 2.43GHz was demonstrated in [7], it utilized a single patch with a size of 30x36 mm<sup>2</sup>. A compact Reconfigurable DRA (Dielectric Resonator Antenna), is presented in [8], and the antenna dimensions are 20×0.8×36mm<sup>3</sup>. Two PIN diodes are utilized to allow the antenna to operate at three different frequency bands: 1.8GHz, 2.6GHz, and 3.6GHz, with bandwidth efficiencies of 11%, 9%, and 19% respectively, the proposed design supports GSM, LTE, and 5G applications.

Paper in [9] Showed a patch design based on u-slots. With a patch element size of 77x57 mm<sup>2</sup>, it provides an adjustable frequency range between 3.35GHz to 2.6GHz. A dual-band stacked patch antenna with two square patches was used to provide frequency reconfigurability between 1.67GHz and 1.92GHz band and between 2.1GHz and 2.5GHz was proposed in [10], each of the square patches was 81x81mm<sup>2</sup> in size. [11] Presented a dual-band slotted patch antenna structure with working frequency bands of (2.22-2.26) GHz and (3.24-4.35) GHz. The square patch piece was 39x39mm<sup>2</sup> in size. [12] proposed a frequency reconfigurable UWB antenna with two tunable rejected band mechanisms, utilizing Varactor diode, to avoid anticipated interference with other systems working within the Ultra Wide Band frequency range; the first notched band may be adjusted from 3.2GHz to 5.1GHz, while the second one is intended to be tuned between 7.25GHz and 9.9GHz. A compact antenna with the embedded slot was presented in [13], the antenna's operating frequency could be reconfigured, using a varactor diode, across a broad frequency range between 2.4 GHz and 1.4GHz to make it suitable for cognitive radio applications. A frequency reconfigurable E-shaped patched antenna with a tuneable frequency range of 2.1GHz to 3.19GHz was reported in [14]. The patch measured 44mm x 92mm in size. An extensive review of reconfigurable patch antennas is presented in [15], with a focus on radiation patterns reconfigurability for the impending 5G Radio frequency bands.

Most frequency reconfigurable patch antennas proposed in the above-mentioned studies employ a single patch antenna element, which is substantial in size and has limited bandwidth. Furthermore, these systems had a restricted frequency tuning range and were unable to accomplish frequency reconfigurability in dual-band employing a reconfigurable feedline. As a result, the goal of this research was to create a compact, frequency-reconfigurable patch antenna with MIMO capabilities.

Multiple-input multiple-output (MIMO) antennas could offer higher data rates by enhancing channel capacity while maintaining the same transmission power. As a result, MIMO antennas are ideal for cognitive radio systems and fourth-generation (4G) cellular communication systems. A thorough analysis of MIMO antenna design techniques for the fifth generation (5G) and beyond is provided in [16]. MIMO performance parameters are thoroughly analysed and provided. A circular array microstrip patch antenna design is proposed in [17]. Millimetre wave technology is used to increase the coverage area. The suggested antenna design performance improved by utilizing MIMO feeding mechanism. The suggested antenna's centre frequency is set at 35 GHz, and its substrate is made of RT-Duroid 5880

material. In [18] a wearable low-profile four-element MIMO antenna was designed and fabricated to operate at the 2.4 GHz ISM band. The suggested antenna has a small size with dimensions of 26mm × 26mm × 0.8mm which is considered one of the smallest available MIMO designs. The designed MIMO revealed strong isolation of about -26 dB at the desired bandwidth. It was also tested on human tissues, and it has been proven to be good for medical systems and WBAN applications.

Many frequencies reconfigurable MIMO antenna designs have been published in [19-21] to incorporate the benefits of MIMO with those of frequency reconfigurable antennas. A frequency reconfigurable MIMO antenna with two ports utilizing compact patch elements operating at the frequency band between 2.11GHz and 2.39GHz was proposed in [19]. [20] Presented a two-port reconfigurable MIMO antenna with a complete metal ringed design structure suitable for WWAN/LTE systems and applications. A four-port reconfigurable MIMO slotted structure for WLAN applications was proposed in [21].

Three radiator elements that have an overall size of 48 mm × 29 mm × 1.6 mm and a narrow BW that is approximately 15% of the operating band 5-6 GHz proposed in [22]. However, this antenna has low gain values at lower bands and low efficiency. The antennas reported in [23], were large and thus cannot be used in modern portable communication devices. Conversely, previous antennas that are small in size also have low efficiency or gain, such as [24,25]. In [26], a four-element dual mode F-shape reconfigurable MIMO antenna is proposed. The reconfigurability is achieved by utilizing a combination of varactor and PIN diodes. The presented design's two modes cover the frequency bands 0.743-1.24 and 2.4 GHz, it utilized a defected ground plane structure to enhance isolation between various antenna elements. [27] presented a 2-element frequency reconfigurable MIMO antenna. The two elements are positioned diagonally to each other to enhance pattern diversity and isolation, two PIN diodes are utilized, per each element, to operate in two switchable frequency bands, 2.4 GHz (LTE) or 3.5 GHz (5G). The proposed MIMO antenna design measured gain values in two modes are 3.7 dBi and 4.2 dBi, respectively with overall efficiency > 60%. A low envelope correlation coefficient (<0.0056) is achieved. A frequency reconfigurable 4-port MIMO antenna is designed and tested for four different 5G bands in [28]. The MIMO elements are made up of two patches. In [29], a reconfigurable 2-element MIMO antenna is presented. A T-shaped stub has been utilized on the ground of the antenna structure to achieve more than 18 dB isolation. In addition, two parasitic elements integrated with 2 PIN diodes, on the ground, are introduced to allow frequency reconfigurability and reduce interference. That allowed the suggested antenna to operate on two frequency bands 3.2-3.8 GHz and 4.95-7 GHz, suitable for 5G and Wi-Fi/WLAN applications.

The antenna designs proposed in this paper are based on the MIMO antenna design proposed in [18] which operates in the ISM band 2.4 GHz. A parametric study has been carried out to change the operating frequency of the proposed design in [18] to 3.5 GHz. After that the 3.5GHz MIMO

antenna has been altered to operate on 5.2GHz, resulting in two new antenna models. The new models were merged in a single reconfigurable MIMO, this first reconfigurable MIMO antenna could be reconfigured to work on both 3.5GHz and 5.2GHz utilizing 4 PIN diodes. A novel balanced feeding concept has been proven and applied to the First reconfigurable antenna proposed in this paper resulting in a Second reconfigurable antenna. The balanced feeding concept has been introduced and applied to the second antenna design mainly to tackle the issue of the small ground.

To facilitate a more effective comparison between the proposed work and other published studies [22-29], Table I summarizes the performance metrics, including compact size, radiation efficiency, ground dependency, and power gain, along with the ECC outcomes. Notably, the proposed Antenna 2 surpasses the others in performance while also demonstrating desirable ground dependency characteristics, making it easy to integrate into future mobile systems.

TABLE I: COMPARISON BETWEEN THE PROPOSED WORK AND OTHER PUBLISHED WORKS.

Ant.	No El.	BW (GHz)	Efficiency %	Gain (dBi)	Ground-Dependent	ECC	S <sub>ij</sub> (dB)	Size (mm)
[22]	3	5-6	55-60	-2 to 2	Yes	0.15	<-15	48x29x1.6
[23]	4	5.1-5.35	-	-	Yes	0.2	<-10	130x10x0.8
[24]	16	5-6	70-80	-	Yes	0.1	<-10	30x30x13
[25]	2	4-6.5	80	4-7	Yes	0.05	<-15	80x50x0.76
[26]	4	1.15-1.22, 0.743-1.24, 2.34-2.46	53, 34, 78	-0.77, 1.798, 3.521	Yes	-	<-6	65x120x1.56
[27]	2	2.2-2.7, 3.3-4.02	70	3.7, 4.2	Yes	0.0056, 0.0009	<-10	120x60x1.52
[28]	4	2.2-2.7, 3.3-3.67, 4.7-5.7	90,77,80	1.75, 1.6, 1.5	Yes	<0.3	<-10	70x70 x1.60
[29]	4	3.2- 3.8, 4.95-7.2	-	4, 5.1	Yes	< 0.02		40x34x0.8
Proposed 1 (3rd design)	4	3.4-3.6 5-5.4	88-80	2.5-3.5	No	0.02, 0.01	<-18	26x26x0.8
Proposed 2 (4th design)	4	3.36-3.7 4.9-5.6	88-91	3.5-4	No	0.0001	<-18	28x28x0.8

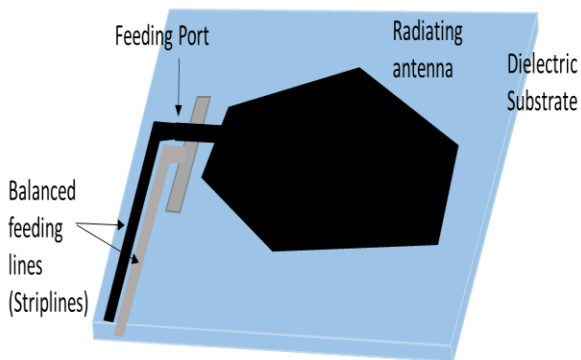


Figure 1: Balanced feeding for radiating element fed at the edge

## II. Antenna Design Methodology

Figure 1 illustrates a planar antenna with its input port positioned near the edge of the dielectric substrate. Numerous studies suggest that enhancing isolation or decoupling the common ground can be achieved by segmenting it into distinct sections on a uniplanar dielectric substrate. However, based on the author's extensive expertise, no effective solutions have been proposed to resolve the issue of ground stability.

As evident from Figure 1, when another antenna is positioned opposite or sufficiently close to the first, one can reasonably expect reduced coupling. Consequently, several previous studies support this observation, as seen in references [30-35]. Most of these works either feature a small ground or one that is not significantly larger than the planar antenna itself, and they often neglect to address the concept of separated ground planes. It is essential to clarify that these ground planes do not involve a defective ground linked to a small piece of conducting material or shorted by passive elements; rather, they are completely separate.

In this antenna design, we have implemented the same above concept to improve the ground stability of the proposed antenna. Three different antenna designs are introduced; the first antenna design operates at 3.5 GHz. The first design is based on the MIMO design proposed in [18]. The ISM 2.4 GHz MIMO antenna presented in [18] is manufactured on an FR-4 substrate (thickness of 0.8 mm, loss tangent of 0.025, and permittivity of 4.3). With a total dimension of 26x26x0.8mm<sup>3</sup>, the suggested shape of the four-element MIMO antenna presented in [18], as shown in Figure 2, could be considered one of the most compacted wearable antenna designs.

Then, the second antenna design is achieved by inserting slots on the radiating elements of the first design. The second antenna design operates at 5.2GHz, the prototype of both MIMO designs depicted in Figure 3. Both designs were

combined in a reconfigurable one using four PIN diodes which were utilized as switches, the PIN diode used is BAR640 2V in CS79 packaging with dimensions  $0.8 \times 0.3 \times 1.2 \text{ mm}^3$ . This third antenna design could be reconfigured to operate at both 3.5GHz and 5.2GHz by changing the switch states. The full configurations of the three designs of four-element multiple-input multiple-output (MIMO) microstrip multi-band patch antennas designs are presented in Figure 4.

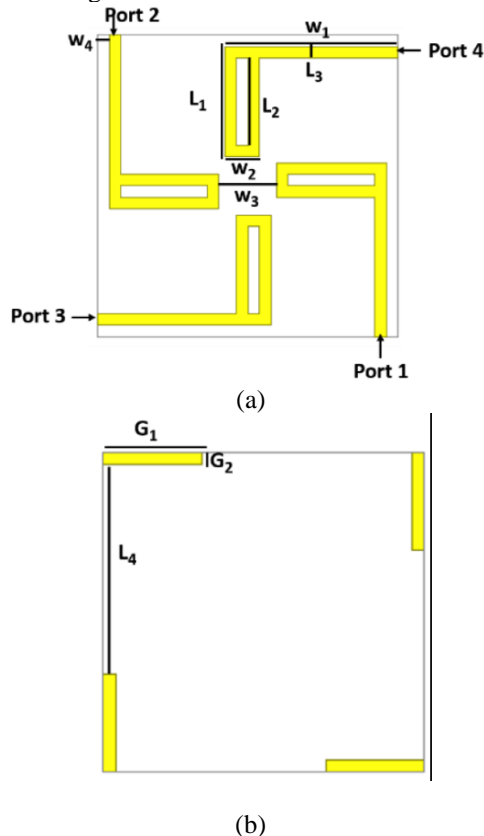


Figure 2: Reference MIMO antenna structure; (a) Top view; (b) ground view

The layout of the proposed design is based on a printed patch radiator. The proposed (3.5, 5.2) GHz reconfigurable MIMO antennas are printed on FR-4 dielectric substrate (permittivity of 4.3, loss tangent of 0.025, and thickness of 0.8 mm) with a size of  $26 \times 26 \times 0.8 \text{ mm}^3$ . As shown in Figure 4 (a, b), each one of the patch antennas consists of two metal planes, the bottom layer being the ground plane  $7.5 \times 1 \text{ mm}^2$  and the top layer is the four-element microstrip MIMO monopole antenna whilst a dielectric material exists between them. These antennas are considered one of the smallest designs in Cognitive radio (CR) antennas with a total size of  $26 \times 26 \times 0.8 \text{ mm}^3$ .

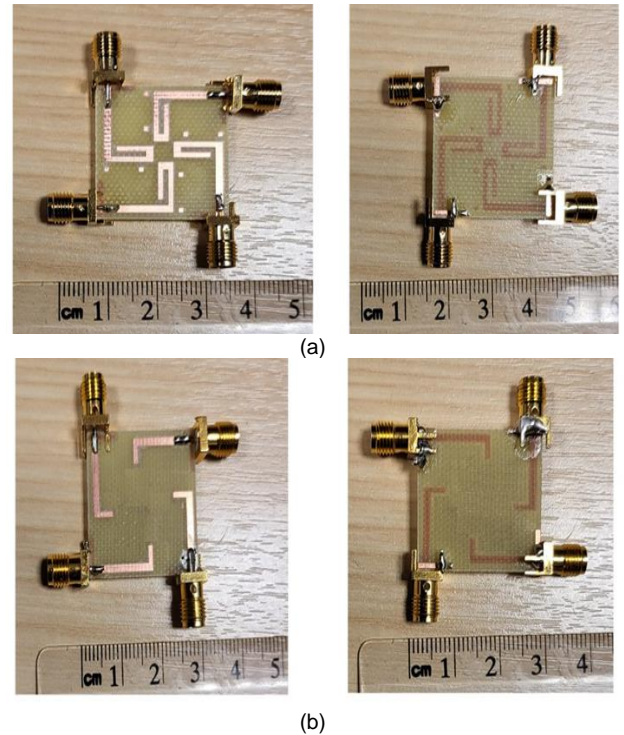
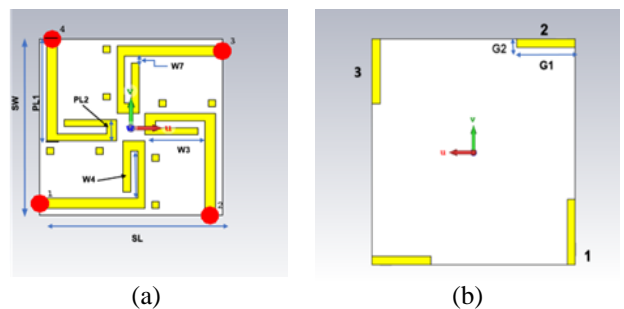


Figure 3: Fabricated prototypes of the two MIMO antennas. Top and bottom view of (a) 3.5 GHz (without slot), (b) 5.2 GHz (with slot)

A 50-Ohm microstrip line is used to feed the proposed antenna. The feed method is chosen due to ease of fabrication and matching. Different optimization methods are carried out to select the optimal location of the feedline. However, there is a significant effect on the antenna reflection coefficient, when the feedline is set at both edges or in the middle.

Therefore, the proposed antenna is fed by four single 50-Ω microstrip lines designed and printed on FR-4 substrate. Initially, four-element antennas were investigated. The dimensions of the antennas were optimized at the desired frequencies at 3.5GHz for the first design, and 5.2GHz for the second design (with engraved slots).

An I-shaped slot is embedded over the surface of each one of the four radiating patches as shown in Figure 4(c). The main objective of the etched slot is to change the resonant frequencies from 3.5GHz to 5.2GHz by using PIN diode to reduce the radiating element size Figure 4(d). The slot has a uniform width of 1mm.



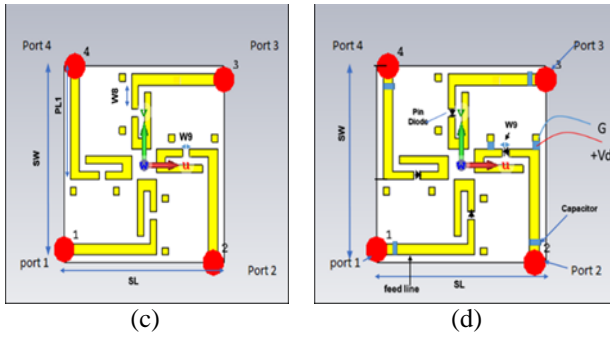


Figure 4: Reconfigurable MIMO antenna proposed structure; (a) Top view; (b) ground view; (c) Top view without diode, (d) Top view with diodes

### A. Switching Mechanism

The PIN diode (BAR640) functions as an electrical switch across any specified frequency range. However, the switching mechanism is distinctive since frequency and pattern reconfigurability are achieved by varying the resonance length, which serves as the control element. The equivalent circuits for using PIN diode in the ON and OFF states are depicted in Figure 5. For the OFF-state, straightforward RLC is created using a capacitor ( $C$ ), a high-value resistor ( $R_H$ ), and a parallel inductor  $L$ . In the ON state, the circuit is reduced to an RL series circuit using an inductor ( $L$ ) and a very low resistor ( $R_L$ ). In the CST simulation software, the parametric values acquired from the PIN diode from the datasheet are modeled as follows:  $R_L = 1.5 \Omega$ ,  $L = 0.7 \text{ nH}$ , and  $C = 0.15 \text{ pF}$ .

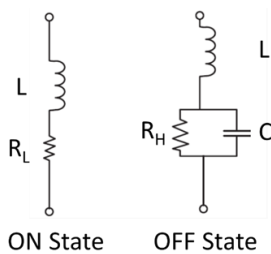


Figure 5: The Equivalent circuit of the PIN diode [37].

### B. First Reconfigurable MIMO Antenna Design

Figure 6 depicts the suggested design, which is composed of 4 identical radiating elements that are symmetrically placed with a separation distance of 3 mm. This is manufactured on an FR-4 substrate (thickness of 0.8 mm, loss tangent of 0.025, and permittivity of 4.3). With a total dimension of  $26 \times 26 \times 0.8 \text{ mm}^3$ , the suggested antenna, as shown in Figure 6(a), is fed through a single  $50 \Omega$  microstrip line developed and manufactured on FR-4 substrate. An I-shaped slot was embedded over the surface of every one of the four radiating elements as shown in Figure 6(a). PIN-diode is loaded in each of the four etched slots to reconfigure the antenna to work at two different frequencies (3.5 GHz, 5.2 GHz). If the PIN diode is switched ON the MIMO antenna will work at 3.5 GHz, and if the diode is OFF the antenna will operate at a frequency of 5.2GHz.

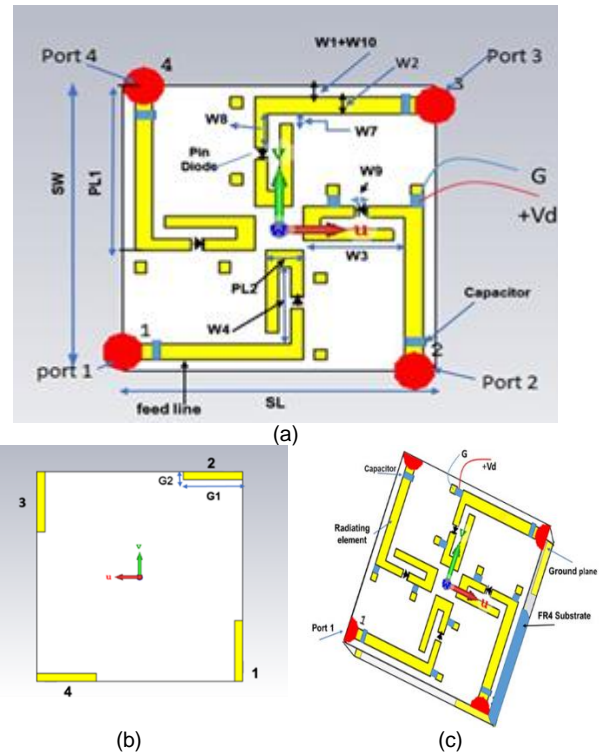


Figure 6: Reconfigurable MIMO antenna structure; (a) Top view; (b) ground view; (c) 3D view

A capacitor is loaded through every one of the four feed line slots to protect the antenna from the DC current. The slot has a uniform width of 1mm. The full dimensions of the top patch are stated in Figure 6(a). The four identical radiating pieces are symmetrically positioned and separated by 3 mm. The extremely tiny ground plane is printed on the lower side of the substrate, as described in [38-40]. The ground plane defected into four rectangle parts printed underneath each radiating element as shown in Figure 6(b).

The schematic views of the considered radiating element (front side) and partial ground (back side) are shown in Figure 6(b, c), along with the optimized dimensions. The present design is simulated with the aid of CST [41]. The detailed geometrical parameters and their sizes are listed in Table II.

A parametric analysis of the antenna geometrical parameters  $W_8$  and  $W_7$  is illustrated in Figure 7. When the PIN diode state is ON performing parametric analysis for  $W_8$ ,  $W_8$  is changed from 3.00 to 3.36 mm in 0.18 mm steps; all other parameters are kept with their nominal values. The stability of the resonance at 5.2 GHz was very strong, as shown in Figure 7(a). Whereas when the PIN diode state is OFF targeting the 3.5 GHz operating frequency,  $W_7$  changes from 2.0 to 2.4 mm in 0.2 mm steps, and all parameters are kept with their nominal values. The stability of the resonance at 3.5 was well reserved, as illustrated in Figure 7b. The optimum values of  $W_8$  and  $W_7$  are considered 3.18 mm, and 2.2 mm, respectively.

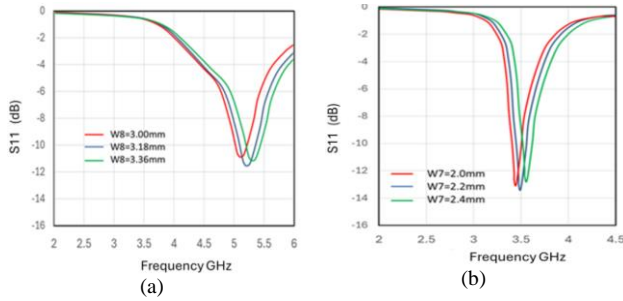


Figure 7: Parametric study of the antenna parameters: (a) W8 and (b) W7

TABLE II: THE DIMENSIONS OF THE FIRST PROPOSED RECONFIGURABLE MIMO ANTENNA

Parameters	Value (mm)	Parameters	Value (mm)
W1	1	PL1	15
W2	1.5	PL2	3.12
W3	8.988	G1	7.5
W4	7	G2	1
W7	2.2	SW	26
W8	3.18	SL	26
W9	1		

Figure 8 depicts the prototype of the four-element reconfigurable MIMO antenna, which was fabricated. Figure 9 shows the antenna inside the anechoic chamber for testing and measurements.

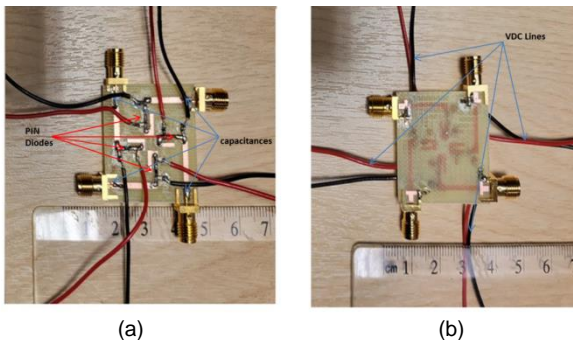


Figure 8: Reconfigurable MIMO fabricated prototype views, (a) Top view and (b) bottom view

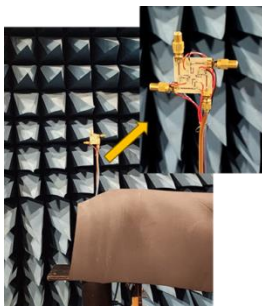


Figure 9: Antenna inside the anechoic chamber for measurement testing  
Figure 10 illustrates the antenna's simulated and measured reflection coefficient in the two operating modes of the PIN

diode (ON/OFF). It could be observed that the resonant frequencies of both the simulated and measured data are in good agreement. The achieved bandwidths are 420 MHz and 120 MHz at the centre frequencies 5.2 GHz and 3.5 GHz respectively.

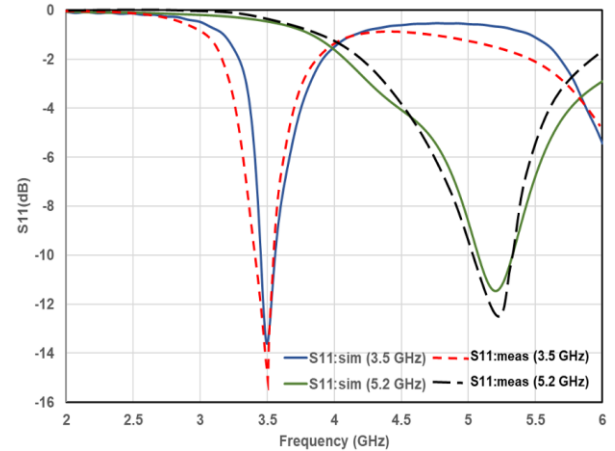


Figure 10: ON and OFF antenna simulated and measured reflection coefficient (S11) In both modes of operation, ON (3.5GHz) and OFF (5.2GHz).

### C. Second (Modified) reconfigurable MIMO antenna Design Methodology

The proposed design of the second reconfigurable MIMO antenna is shown in Figure 11, The new proposed design is based on the reconfigurable antenna design we mentioned before in Figure 6 with some enhancements, this antenna is also composed of four identical radiating elements symmetrically placed with a separation distance of 3 mm. It is fabricated utilizing FR-4 substrate (thickness of 0.8 mm, loss tangent of 0.025, and permittivity of 4.3).

By using the balanced feeding network concept presented in section II, two parallel lines were introduced on each of the four ports. One of them (the parallel lines) is connected to the feeding line in each port (top side of the substrate), while the other parallel line is connected to the ground of each port (bottom side of the substrate), as shown in Figure 11(b, c). in order to maintain the operating frequencies of the antenna a parametric study was performed to get the optimum size of each of parallel lines  $1.5 \times 2 \text{ mm}^2$ , it is worth mentioning that the lines are made of the same radiating element material. As a result of introducing the above-mentioned lines, the size of the new antenna has changed to  $28 \times 28 \times 0.8 \text{ mm}^3$ , which is still considered very small. Two slots were embedded over the surface of every one of the four radiating elements. The slots have a uniform width of 1 mm for the first slot and the second one is 0.5 mm. A 50 pF capacitor is loaded, for DC biasing purposes. The full dimensions of the top patch are stated in Figure 11(a). Table III shows all the detailed geometrical parameters of the proposed modified antenna.

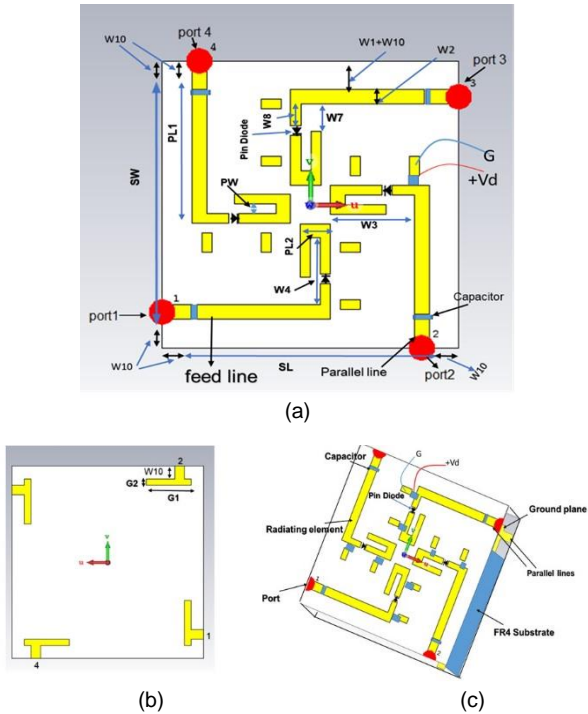


Figure 11: Modified (Enhanced) reconfigurable MIMO antenna structure; (a) Top view; (b) ground view; (c) 3D view antenna.

TABLE III: THE DIMENSIONS OF THE MODIFIED RECONFIGURABLE MIMO ANTENNA

Parameters	Value (mm)	Parameters	Value (mm)
W1	1	PL1	15
W2	1.5	PL2	3.05
W3	8.98	G1	7
W4	7	G2	1
W7	2.85	SW	26
W8	2.25	SL	26
W9	1	W10	2

Figure 12 shows the prototype of the Modified reconfigurable four-element MIMO antenna, which was fabricated. Figure 13 depicts the antenna's simulated and measured reflection coefficient in both switching configurations (ON: 3.5GHz, OFF: 5.2GHz). It could be observed from Figure 13 that the resonant frequencies of both the simulated and measured data are in good agreement. Also, the fabricated prototype's measured bandwidth is less than the simulated one, but it is yet larger than the intended WiFi and WLAN bands.

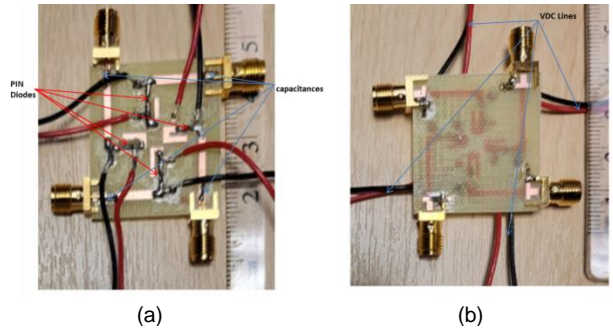


Figure 12: The Enhanced (Modified) reconfigurable MIMO antenna fabricated prototype views, (a) Top view and (b) bottom view

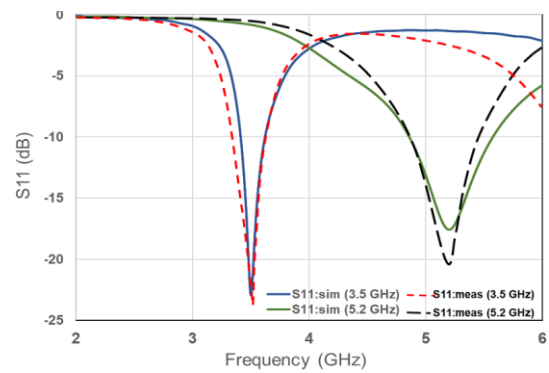


Figure 13: The Modified antenna simulated and measured loss S11 return for both switching configurations ON (3.5GHz) and OFF (5.2GHz).

### III. EFFECT OF REFLECTION COEFFICIENT OF THE PROPOSED ANTENNA

The above-mentioned antennas (with and without slots) offer some advantages including size miniaturization and operating between two important resonant frequencies of LTE and WLAN. However, these two resonant frequencies are fixed and cannot be altered/tuned once the antenna is fabricated, and this may not be considered attractive for the cognitive radio system. Thus, in the first instance, a PIN diode is attached over the I-shaped slot of the first and second antenna as shown in Figure 6 and Figure 11, the I-shaped slot antenna along with a PIN diode and a suitable DC bias circuit is further explored as shown in Figure 6 and Figure 11.

The loaded PIN diode operates as a switch to control the antenna operating modes; both frequency coefficient and bandwidth were improved compared with the first reconfigurable MIMO antenna design, either at 3.5 GHz if the switch is ON, or at 5.2 GHz if the switch is OFF. A 100nH inductor is utilized to control the current flowing to the PIN diode. Two capacitors with a value of 50 pF are attached to the ends of each of the feeding lines for DC biasing. Figure 14 shows that by comparing the two antennas when the diode was inserted over an accurate location of the slot, the proposed design achieved the targeted frequencies 3.5 GHz and 5.2 GHz, while in the second antenna, both the reflection coefficient and the bandwidth were improved compared with first reconfigurable MIMO antenna design.

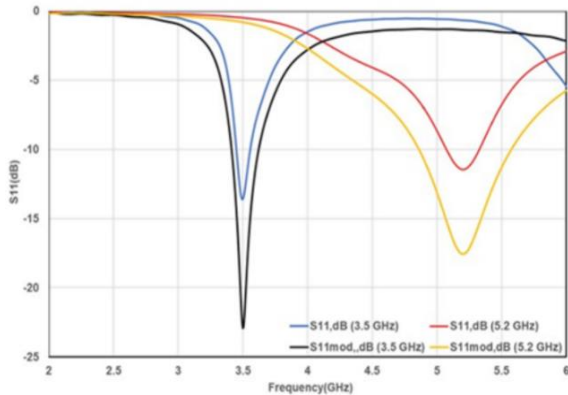
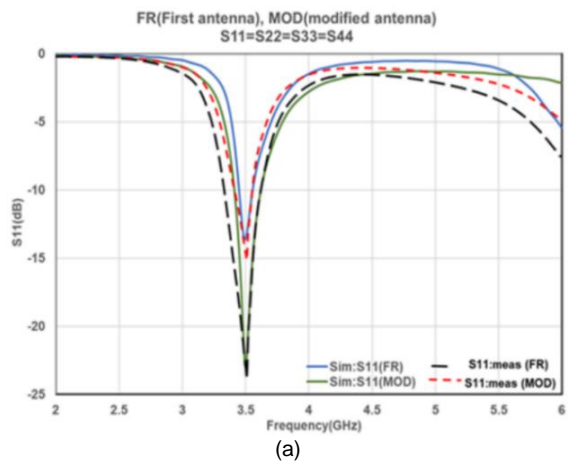


Figure 14: Comparing the reflection coefficient S11 of both the First and Modified Reconfigurable MIMO antennas.

#### IV. COMPARISON OF SIMULATION WITH MEASURED RESULT

The First and the Modified four-element MIMO antenna models were fabricated to validate the simulated designs, as shown in Figure 8 and Figure 12 respectively. The MIMO antennas were constructed on a 0.8 mm thick FR-4 substrate. To create the antennas' partial ground planes, a rectangular copper component was printed beneath each of the four radiating elements. As seen in Figure 8 and Figure 12, SMA connectors were used to feed each of the four radiating elements. The measured and simulated s-parameters of the designed MIMO antenna are in line with each other as shown in both Figure 10 and Figure 13. Figure 15 shows the simulated and measured s-parameters of both MIMO antennas (First/Modified). The modified reconfigurable MIMO antenna has a -10 dB impedance bandwidth at the 3.5GHz (5G) and 5.2GHz (WiFi) bands, where the operating frequency is from 3.3 to 3.6GHz at a centre frequency 3.5GHz and from 4.7 to 5.45GHz at a centre frequency 5.2GHz. The reflection coefficients achieved were -24dB and -21dB at centre frequencies of 3.5GHz and 5.2GHz respectively.



(a)

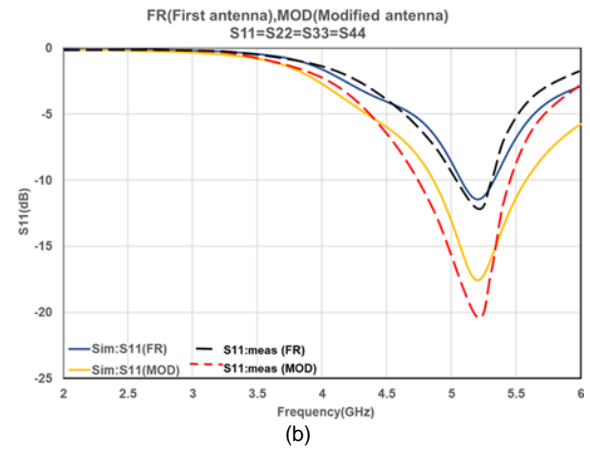
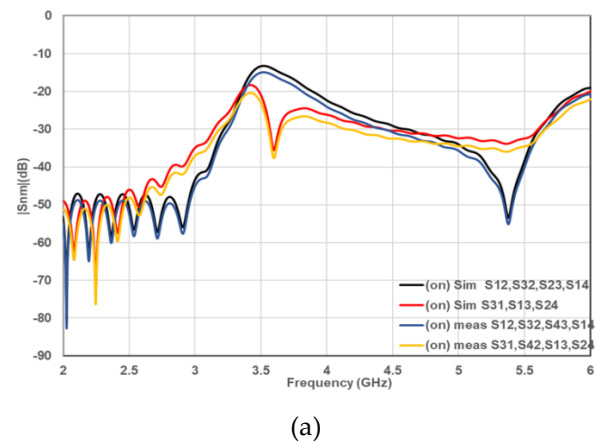


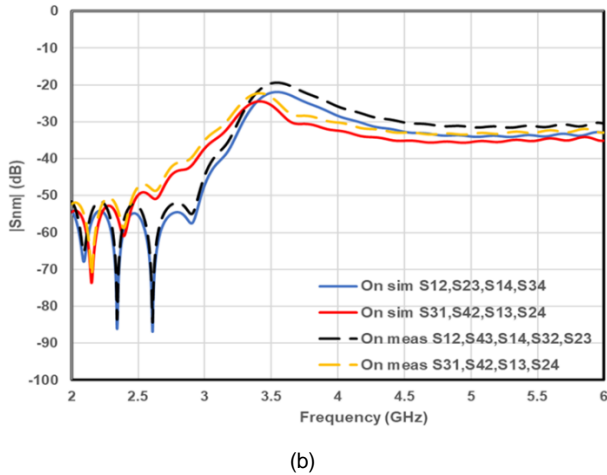
Figure 15: Comparing the s-parameters of the simulated models and fabricated prototypes of both First and Modified reconfigurable MIMO antennas (a) 3.5 GHz and (b) 5.2 GHz

The isolation between the four radiating elements of both reconfigurable MIMO antenna designs was investigated and analysed to further study the antenna's diversity performance that is because the isolation has a direct relation with the minimal coupling between the four antenna radiating elements in both of the designed antennas. Figure 16 and Figure 17 depict the measured and simulated isolation results between radiating antenna elements in both designs (first/modified). In the targeted antenna's impedance bandwidth, the isolation values range for the first antenna was from -13 dB to -22dB at 3.5 GHz, and they are between -18dB and -25dB at 5.2 GHz. While in the second antenna, the isolation values were between -20dB and -26dB at 3.5 GHz, and from -18dB to -30dB at 5.2 GHz. The results suggest that the measured and the simulated results were close, and the coupling between the four elements was less. That means the isolation obtained results are adequate for MIMO systems operating at 5G and Wi-Fi wireless applications.



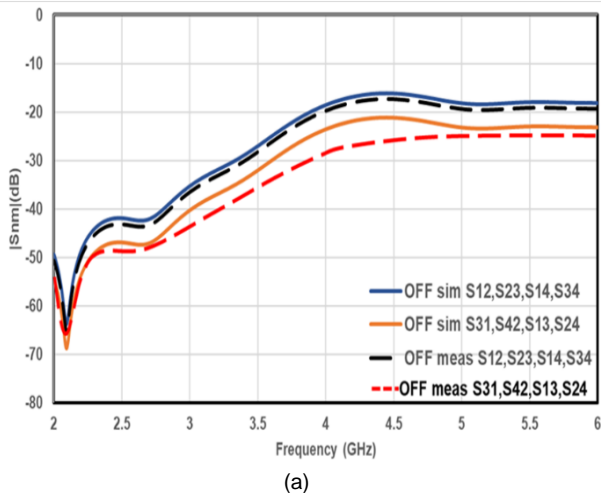
(a)



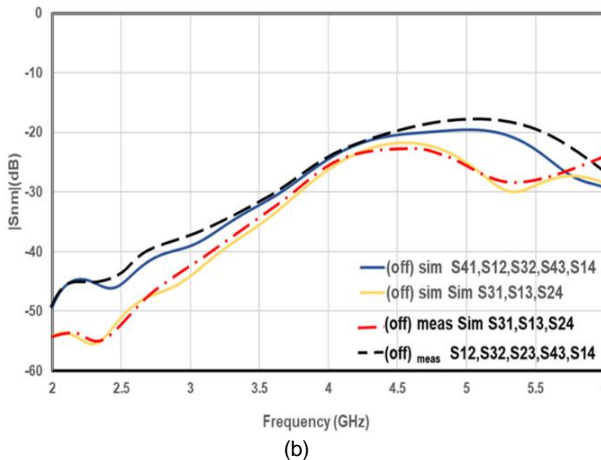


(b)

Figure 16: Simulated and measured isolation results of the designed antennas when the switch configuration is ON at 3.5 GHz, (a) First antenna, (b) Modified antenna.



(a)



(b)

Figure 17: Simulated and measured isolation results of the designed antennas when the switch configuration is OFF at 5.2 GHz, (a) First antenna, (b) Modified antenna.

## V. DISTRIBUTION OF CURRENT ON BOTH THE FIRST ANTENNA AND MODIFIED ANTENNA SURFACES AND THEIR RADIATION PATTERN

The MIMO antenna surface current, as shown in Figure 18, may be used to confirm the results of the mutual coupling between the radiating elements of the designed MIMO antenna illustrated in Figure 15, Figure 16, and Figure 17. In general, one of the four ports should be stimulated to understand the impact of the coupling between the antenna parts, while the other remaining ports should be terminated by a  $50 \Omega$  load; this strategy was used as demonstrated in Figure 18. The distance between the four ports is regarded as an essential element in determining how well the isolation between the antennas is. Usually, when the antenna elements are far apart, there is a high level of isolation.

Figure 18 shows that when one port is activated, the remaining ports are terminated with a load of  $50 \Omega$ . As seen in Figure 18(a), the greater current value in the first antenna is concentrated on the top part of the radiating element whereas the modified antenna was distributor on both of the radiating element and the feeding strip since there is no current coupled to the neighboring ports. From Figure 18 (b) the greater current value in the first antenna is focused on the feeding strip of the radiating element, whereas in the modified antenna the current was distributor on the booth of the radiating element and the feeding strip since there is no current coupled to the neighboring ports. As a result, its influence is seen in terms of the isolation parameter S12 or S34. In the case of port 2 being excited and the others being terminated, the current exists solely on this port and is insignificant on the other three as shown in Figure 18(a, b) in both antennas. A similar situation is seen when only ports 3 and 4 are stimulated.

Figure 18(a, b) shows that the surface current is mostly centered over the port that is been excited. Accordingly, the measured and simulated isolations for the designed MIMO antennas in Figure 15, Figure 16, and Figure 17 are greater than 10 dB for both antennas. In addition, we can see from Figure 18(a, b) that the current surface level is higher, and its distribution on the radiating element is clearer in the modified antenna compared with the first antenna, especially at 3.5 GHz.

At the centre frequencies of 3.5 and 5.2 GHz, two planes, H-plane and E-plane, are used to investigate the radiation patterns of the proposed antennas, as shown in Figure 19, it was done by exciting one port and loading the remaining ones by  $50 \Omega$ . As previously stated, the current MIMO antennas H and E plane simulated field patterns are displayed at the 3.5 GHz and 5.2 GHz (5G and Wi-Fi Bands) resonant frequencies.

The radiation is observed and recorded within an anechoic chamber. A standard horn antenna is used as a transmitter. During the measurement procedure, one port is designated to function as a receiver, while the other ports are terminated using  $50 \Omega$  to avoid signal pick-up. This method is done for each port of the two designed antennas in sequence. Figure 19 compares both the (CST) simulated and (prototype)

measured radiation patterns of the First and Modified reconfigurable MIMO antennas. The modified reconfigurable antenna would be suitable for use in communication systems due to its symmetric shape, which aids in achieving a steady radiation pattern. Certain discrepancies between the measured and simulated radiation patterns are discovered, which may be attributable to cable/port losses and flaws in the manufacturing process.

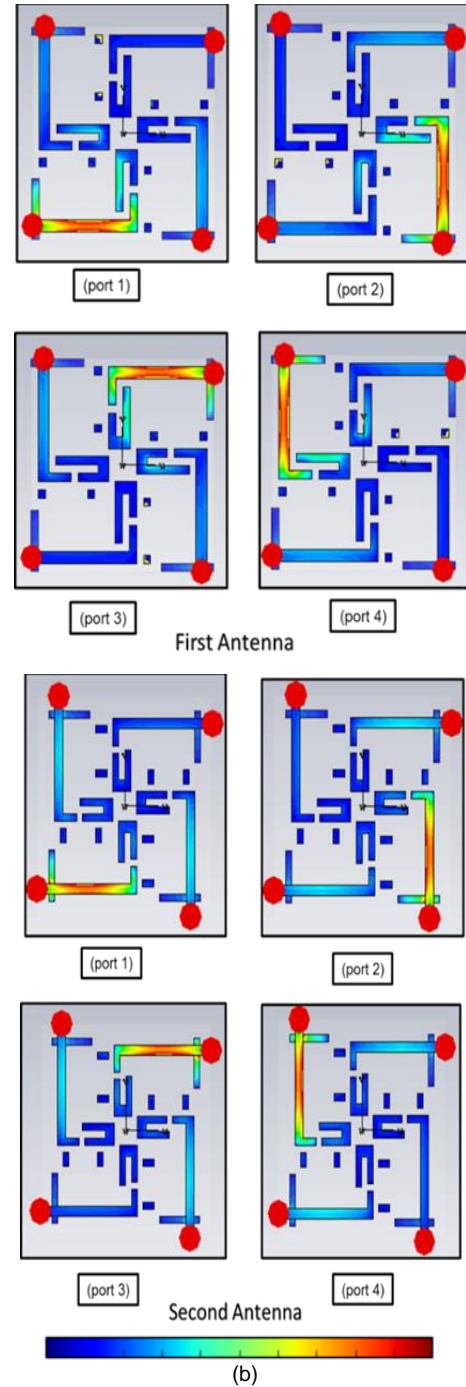
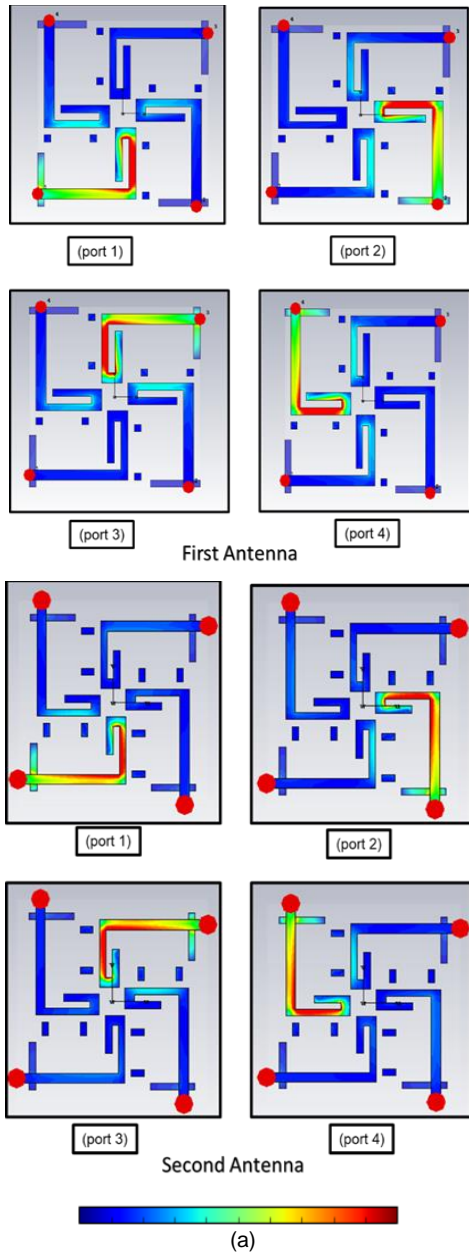


Figure 18: The surface current distribution of the First and Modified reconfigurable MIMO antennas at (a) 3.5 GHz, and (b) 5.2 GHz.

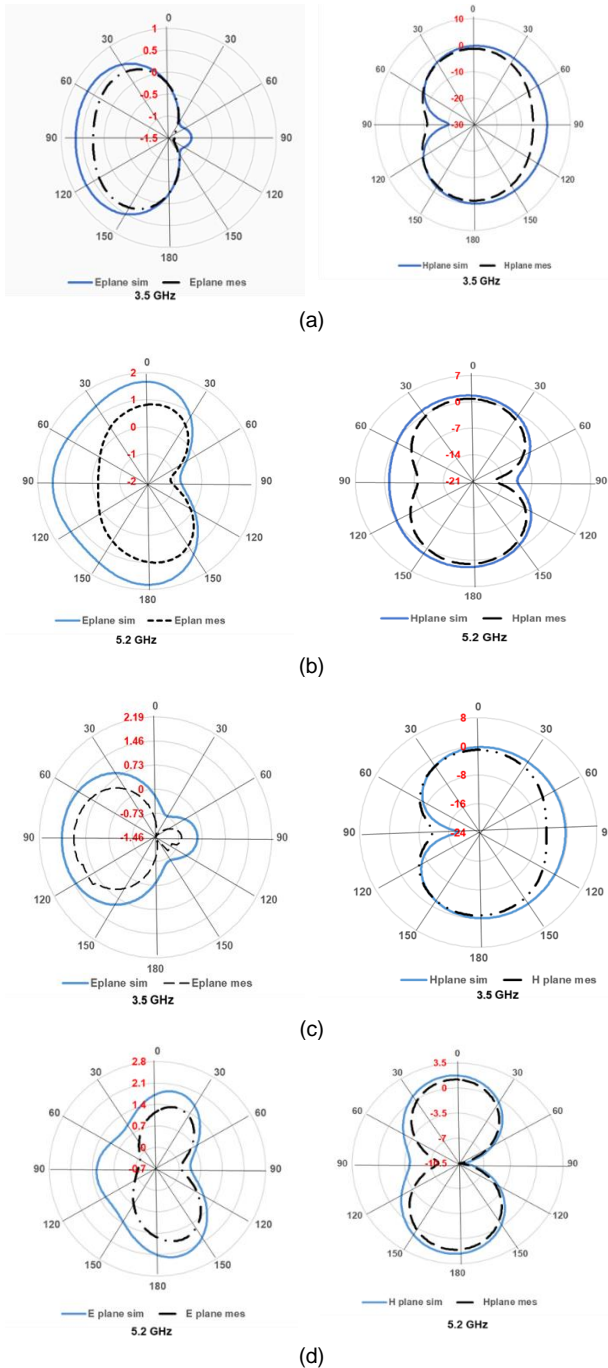


Figure 19: Simulated and measured radiation patterns of the proposed Reconfigurable MIMO antennas designs for port one, (a, b) First antenna, (c, d) Modified antenna.

## VI. Investigating the antenna performance.

One of the key parameters of an antenna is its gain. The gain of a MIMO antenna is considered a far-field parameter, and it is measured using a traditional horn antenna as a transmitter and the antenna to be tested as a receiver, in an anechoic chamber. From Figure 20 (a, b), the peak value of the measured and simulated gain for the first antenna varies between 2.25 dBi and 2.55 dBi at a frequency of 3.5 GHz,

and between 2.9 dBi and 3.11 dBi at a frequency of 5.2 GHz. Whereas in the second antenna (modified one), the gain varies between 3.8 dBi and 4 dBi at a frequency of 3.5 GHz, and between 3.97 dBi and 4.15 dBi at a frequency of 5.2 GHz.

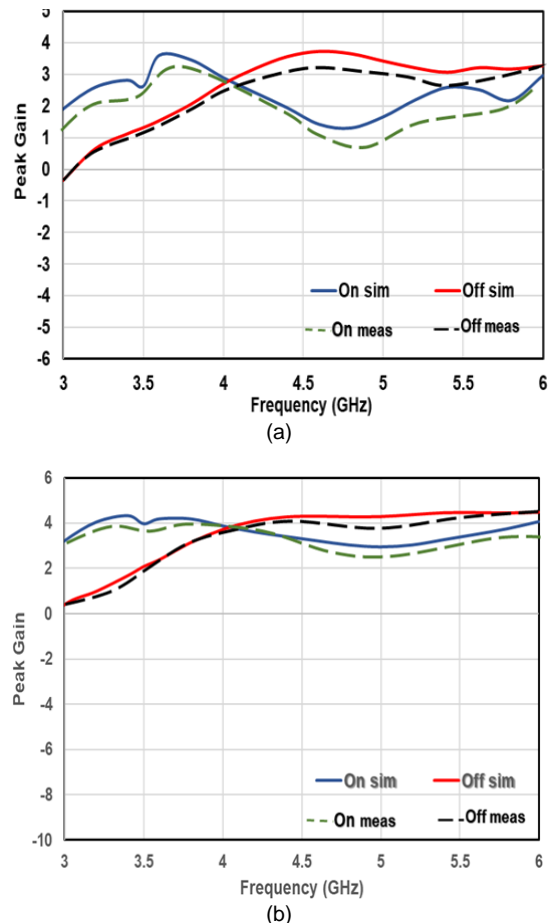


Figure 20: The gain (measured/simulated) results of the First and the Modified reconfigurable MIMO antennas at ON(3.5GHz)/OFF(5.2GHz) switch configuration: (a) First antenna, (b) Second antenna (modified antenna)

The gain of both fabricated antenna prototypes the first and the modified reconfigurable MIMO antennas was measured, at the same frequency bands is around (2.5 dBi at 3.5 GHz, 3 dBi at 5.2 GHz) for the first antenna. Whereas the modified one was around (3.5 dBi at 3.5 GHz, and 4 dBi at 5.2 GHz). The measured and simulated gain results are in agreement. By comparing both of these antenna results it could be clearly seen how the peak gain improved after the first antenna was modified.

The computed Envelope Correlation Coefficient (ECC) between the four ports of the MIMO antenna structure in both frequencies (3.5 GHz, 5.2 GHz), on the first antenna and in the second one, is displayed in Figure 21(a, b). In terms of the radiation pattern, the ECC of the MIMO system depicts how independent the four elements are. Each of the four elements in a MIMO system should always be independent of the other three. Taking into consideration that all four antenna elements of the two proposed MIMO systems are identical, it is only fair to say that;  $S_{12} = S_{21} =$

$S_{14} = S_{41} = S_{23} = S_{32} = S_{34} = S_{43}$ , and  $S_{13} = S_{31} = S_{24} = S_{42}$ , while  $S_{11} = S_{22} = S_{33} = S_{44}$ , the ECC values of element one may be obtained in this situation by substituting the necessary terms into the following Equations 1, 2 and 3:

$$\rho_{e12} = \frac{|s_{11}^*s_{12} + s_{11}^*s_{22} + s_{13}^*s_{32} + s_{14}^*s_{42}|^2}{(1 - (|s_{11}|^2 + (|s_{12}|^2(|s_{13}|^2 + (|s_{14}|^2)^2)))^2} \quad (1)$$

$$\rho_{e13} = \frac{|s_{11}^*s_{13} + s_{11}^*s_{23} + s_{13}^*s_{33} + s_{14}^*s_{43}|^2}{(1 - (|s_{11}|^2 + (|s_{12}|^2(|s_{13}|^2 + (|s_{14}|^2)^2)))^2} \quad (2)$$

$$\rho_{e14} = \frac{|s_{11}^*s_{14} + s_{11}^*s_{24} + s_{13}^*s_{34} + s_{14}^*s_{44}|^2}{(1 - (|s_{11}|^2 + (|s_{12}|^2(|s_{13}|^2 + (|s_{14}|^2)^2)))^2} \quad (3)$$

Figure 21 shows that the ECC between the four ports of the MIMO system for the band (3.5GHz, 5.2GHz) in the first antenna is approximately less than (0.02, 0.01) whereas for the second antenna was about 0.0001 on both operating frequencies. As a result, this ECC value is tolerable and comparable to those found in [42], showing positive performance.

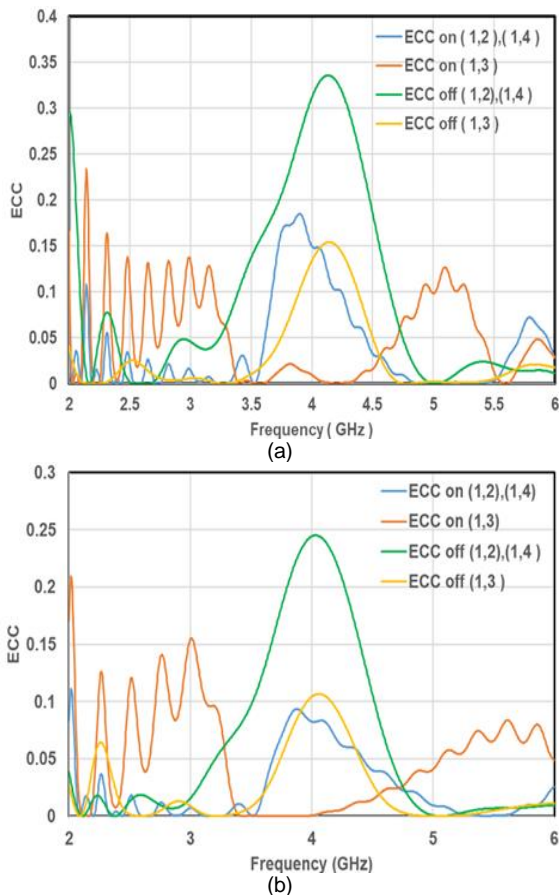


Figure 21: ECC (Envelope Correlation Coefficient), (a) first antenna, (b) modified antenna

Any diversity technique that improves the signal-to-interference ratio is known as diversity gain. It is regarded as

a crucial diversity parameter [43]. The diversity gain might be calculated using Equations 16, 17, and 18 using the correlation coefficient. Because the antenna has a larger diversity gain value, it achieves better isolation and the other way around. Figure 22 shows the investigation of the diversity gain (DG) of the First reconfigurable MIMO antenna as well as in the modified one. The DG values for both scenarios are around 10 dB at the antenna operational bandwidth.

$$DG_{12} = 10\sqrt{1 - |\rho_{e12}|^2} \quad (4)$$

$$DG_{13} = 10\sqrt{1 - |\rho_{e13}|^2} \quad (5)$$

$$DG_{14} = 10\sqrt{1 - |\rho_{e14}|^2} \quad (6)$$

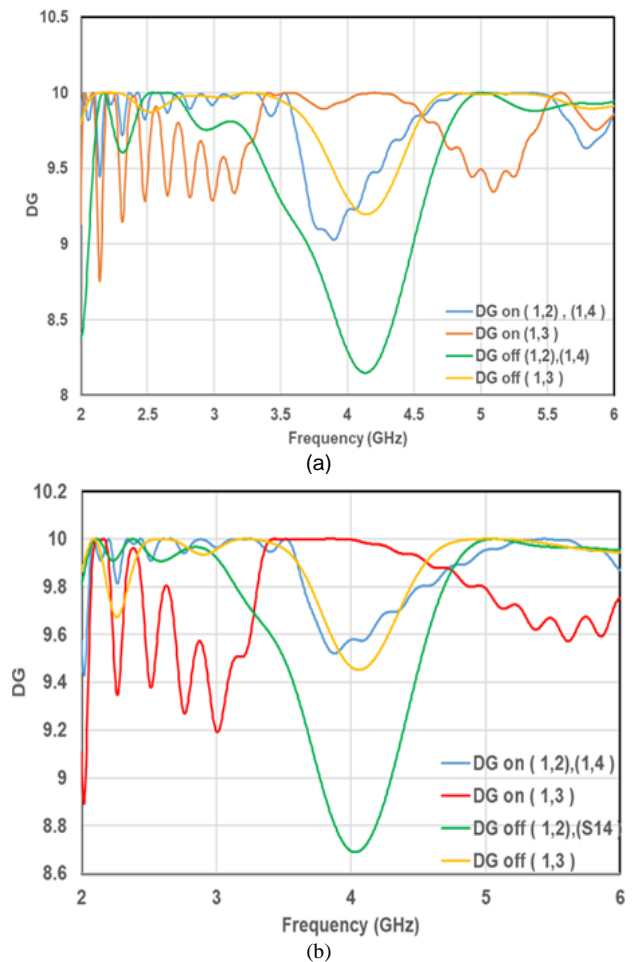


Figure 22: Diversity Gain of the two proposed antennas, (a) First antenna, (b) Modified antenna.

The efficiency of the proposed MIMO antenna also is a major characteristic of its diverse behavior. Figure 23 shows that the radiation efficiencies over the targeted 3.5 GHz and 5.2 GHz Wi-Fi bands in the First antenna design are about

80% at 3.5 GHz and 88% at 5.2 GHz, while in the Modified antenna is about 88% at 3.5 GHz and 91% at 5.2 GHz.

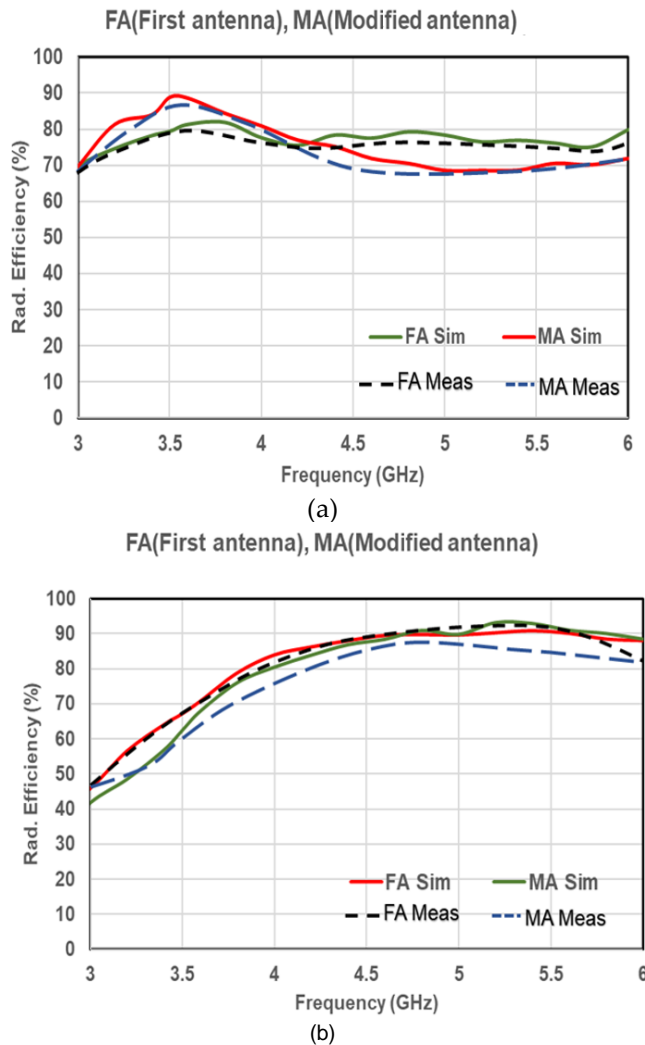


Figure 23: Antenna radiation efficiencies Simulated and measured results, for the first and Modified reconfigurable MIMO antennas at frequencies (a) 3.5 GHz, (b) 5.2 GHz.

## VII. CONCLUSIONS

In conclusion, the four miniaturized MIMO antenna designs proposed in this study demonstrate excellent performance in terms of impedance matching, isolation, ECC, DG, peak realized gains, and radiation efficiency at both 3.5 GHz and 5.2 GHz frequencies. The new concept of balance introduced in the third and fourth designs addresses the issue of small ground and further improves the overall performance of the antennas. The measured results validate the effectiveness of the designs, showing good agreement with simulation results. Overall, these compact and reconfigurable MIMO antennas offer promising potential for various wireless communication applications.

## ACKNOWLEDGMENT

This work is partially supported by the UK Engineering and Physical Sciences Research Council (EPSRC) under grant EP/Y035135/1, and HORIZON-MSCA-2022-SE-01-01-ID: 101131501, Marie Skłodowska-Curie, Research and Innovation Staff Exchange (RISE), titled: 6G Terahertz Communications for Future Heterogeneous Wireless Network (6G-TERAFIT).

## REFERENCES

1. C. G. Christodoulou, Y. Tawk, S. A. Lane, and S. R. Erwin, 'Reconfigurable Antennas for Wireless and Space Applications', *Proceedings of the IEEE*, vol. 100, no. 7, pp. 2250–2261, Jul. 2012, doi: 10.1109/JPROC.2012.2188249.
2. M. U. Khan, M. S. Sharawi, and R. Mittra, 'Microstrip patch antenna miniaturisation techniques: a review', *IET Microwaves, Antennas & Propagation*, vol. 9, no. 9, pp. 913–922, Jun. 2015, doi: 10.1049/iet-map.2014.0602.
3. C. Zebiri *et al.*, 'A compact frequency reconfigurable DRA for GSM, LTE, and 5G applications services', in *2020 14th European Conference on Antennas and Propagation (EuCAP)*, IEEE, Mar. 2020, pp. 1–5. doi: 10.23919/EuCAP48036.2020.9135747.
4. Y. Tawk, J. Costantine, A. H. Ramadan, K. Y. Kabalan, and C. G. Christodoulou, 'A reconfigurable feeding network', in *The 8th European Conference on Antennas and Propagation (EuCAP 2014)*, IEEE, Apr. 2014, pp. 1534–1536. doi: 10.1109/EuCAP.2014.6902075.
5. H. A. Majid, M. K. Abd Rahim, M. R. Hamid, and M. F. Ismail, 'FREQUENCY RECONFIGURABLE MICROSTRIP PATCH-SLOT ANTENNA WITH DIRECTIONAL RADIATION PATTERN', *Progress In Electromagnetics Research*, vol. 144, pp. 319–328, 2014, doi: 10.2528/PIER13102901.
6. H. A. Majid, M. K. Abdul Rahim, M. R. Hamid, N. A. Murad, and M. F. Ismail, 'Frequency-Reconfigurable Microstrip Patch-Slot Antenna', *IEEE Antennas Wirel Propag Lett*, vol. 12, pp. 218–220, 2013, doi: 10.1109/LAWP.2013.2245293.
7. M. S. Khan, A. Iftikhar, A.-D. Capobianco, R. M. Shubair, and B. Ijaz, 'Pattern and frequency reconfiguration of patch antenna using PIN diodes', *Microw Opt Technol Lett*, vol. 59, no. 9, pp. 2180–2185, Sep. 2017, doi: 10.1002/mop.30709.
8. J. Kosha *et al.*, 'Reconfigurable Dielectric Resonator Antenna for GSM, LTE, and 5G applications', in *Proceedings of the Proceedings of the 1st International Multi-Disciplinary Conference Theme: Sustainable Development and Smart Planning, IMDC-SDSP 2020, Cyberspace, 28-30 June 2020*, EAI, 2020. doi: 10.4108/eai.28-6-2020.2298076.
9. S.-L. S. Yang, A. A. Kishk, and Kai-Fong Lee, 'Frequency Reconfigurable U-Slot Microstrip Patch Antenna', *IEEE Antennas Wirel Propag Lett*, vol. 7, pp. 127–129, 2008, doi: 10.1109/LAWP.2008.921330.
10. L. Ge, M. Li, J. Wang, and H. Gu, 'Unidirectional Dual-Band Stacked Patch Antenna With Independent

- Frequency Reconfigurable', *IEEE Antennas Wirel Propag Lett*, vol. 16, pp. 113–116, 2017, doi: 10.1109/LAWP.2016.2558658.
11. A. Khidre, F. Yang, and A. Z. Elsherbeni, 'A Patch Antenna With a Varactor-Loaded Slot for Reconfigurable Dual-Band Operation', *IEEE Trans Antennas Propag*, vol. 63, no. 2, pp. 755–760, Feb. 2015, doi: 10.1109/TAP.2014.2376524.
  12. I. Elfergani, J. Rodriguez, I. Otung, W. Mshwat, and R. Abd-Alhameed, 'Slotted Printed Monopole UWB Antennas with Tunable Rejection Bands for WLAN/WiMAX and X-Band Coexistence', *Radioengineering*, vol. 27, no. 3, pp. 694–702, Sep. 2018, doi: 10.13164/re.2018.0694.
  13. I. T. E. Elfergani *et al.*, 'Reconfigurable Microstrip Printed Patch Antenna for Future Cognitive Radio Applications', *EAI Endorsed Transactions on Cognitive Communications*, vol. 3, no. 12, p. 153473, Dec. 2017, doi: 10.4108/eai.13-12-2017.153473.
  14. H. Rajagopalan, J. M. Kovitz, and Y. Rahmat-Samii, 'MEMS Reconfigurable Optimized E-Shaped Patch Antenna Design for Cognitive Radio', *IEEE Trans Antennas Propag*, vol. 62, no. 3, pp. 1056–1064, Mar. 2014, doi: 10.1109/TAP.2013.2292531.
  15. S. R. Isa *et al.*, 'Reconfigurable pattern patch antenna for mid-band 5G: A review', *Computers, Materials and Continua*, vol. 70, no. 2, pp. 2699–2725, 2022, doi: 10.32604/cmc.2022.019769.
  16. T. Raj, R. Mishra, P. Kumar, and A. Kapoor, 'Advances in MIMO Antenna Design for 5G: A Comprehensive Review', *Sensors*, vol. 23, no. 14, p. 6329, Jul. 2023, doi: 10.3390/s23146329.
  17. H. V. Pallavi, A. P. J. Chandra, and Paramesha, '5G wireless communication microstrip patch antenna array design with MIMO', *Multimed Tools Appl*, vol. 82, no. 20, pp. 31129–31155, Aug. 2023, doi: 10.1007/s11042-023-14628-2.
  18. I. Elfergani *et al.*, 'Low-Profile and Closely Spaced Four-Element MIMO Antenna for Wireless Body Area Networks', *Electronics (Basel)*, vol. 9, no. 2, p. 258, Feb. 2020, doi: 10.3390/electronics9020258.
  19. A. Raza, M. U. Khan, R. Hussain, F. A. Tahir, and M. S. Sharawi, 'A 2-element reconfigurable MIMO antenna consisting of miniaturized patch elements', in *2016 IEEE International Symposium on Antennas and Propagation (APSURSI)*, IEEE, Jun. 2016, pp. 655–656. doi: 10.1109/APS.2016.7696036.
  20. Z.-Q. Xu, Y.-T. Sun, Q.-Q. Zhou, Y.-L. Ban, Y.-X. Li, and S. S. Ang, 'Reconfigurable MIMO Antenna for Integrated-Metal-Rimmed Smartphone Applications', *IEEE Access*, vol. 5, pp. 21223–21228, 2017, doi: 10.1109/ACCESS.2017.2757949.
  21. S. Soltani, P. Lotfi, and R. D. Murch, 'A Port and Frequency Reconfigurable MIMO Slot Antenna for WLAN Applications', *IEEE Trans Antennas Propag*, vol. 64, no. 4, pp. 1209–1217, Apr. 2016, doi: 10.1109/TAP.2016.2522470.
  22. Y. Sharma, D. Sarkar, K. Saurav, and K. V. Srivastava, 'Three-Element MIMO Antenna System With Pattern and Polarization Diversity for WLAN Applications', *IEEE Antennas Wirel Propag Lett*, vol. 16, pp. 1163–1166, 2017, doi: 10.1109/LAWP.2016.2626394.
  23. G. Brzezina, A. A. Basri, A. Ghasemi, J. Sydor, and A. Vukovic, 'Design and analysis of a low-profile directive antenna array for multi-element terminals', *IET Microwaves, Antennas & Propagation*, vol. 8, no. 8, pp. 611–620, Jun. 2014, doi: 10.1049/iet-map.2013.0459.
  24. M. V. Komandla, G. Mishra, and S. K. Sharma, 'Investigations on Dual Slant Polarized Cavity-Backed Massive MIMO Antenna Panel With Beamforming', *IEEE Trans Antennas Propag*, vol. 65, no. 12, pp. 6794–6799, Dec. 2017, doi: 10.1109/TAP.2017.2748239.
  25. S. S. Jehangir and M. S. Sharawi, 'A Miniaturized UWB Biplanar Yagi-Like MIMO Antenna System', *IEEE Antennas Wirel Propag Lett*, vol. 16, pp. 2320–2323, 2017, doi: 10.1109/LAWP.2017.2716963.
  26. R. Hussain and M. S. Sharawi, '4-element planar MIMO reconfigurable antenna system for cognitive radio applications', in *IEEE Antennas and Propagation Society, AP-S International Symposium (Digest)*, Institute of Electrical and Electronics Engineers Inc., Oct. 2015, pp. 717–718. doi: 10.1109/APS.2015.7304745.
  27. A. Pant, M. Singh, and M. S. Parihar, 'A frequency reconfigurable/switchable MIMO antenna for LTE and early 5G applications', *AEU - International Journal of Electronics and Communications*, vol. 131, Mar. 2021, doi: 10.1016/j.aeue.2021.153638.
  28. G. Singh *et al.*, 'Frequency Reconfigurable Quad-Element MIMO Antenna with Improved Isolation for 5G Systems', *Electronics (Basel)*, vol. 12, no. 4, p. 796, Feb. 2023, doi: 10.3390/electronics12040796.
  29. R. K. Verma, A. Kumar, and R. L. Yadava, 'Wi-fi reconfigurable dual band microstrip mimo antenna for 5g and wi-fi wlan applications', *Przeegląd Elektrotechniczny*, vol. 97, no. 7, pp. 66–71, 2021, doi: 10.15199/48.2021.07.13.
  30. S. Agarwal, U. Rafique, R. Ullah, S. Ullah, S. Khan, and M. Donelli, 'Double Overt-Leaf Shaped CPW-Fed Four Port UWB MIMO Antenna', *Electronics (Basel)*, vol. 10, no. 24, p. 3140, Dec. 2021, doi: 10.3390/electronics10243140.
  31. Z. Tang, X. Wu, J. Zhan, S. Hu, Z. Xi, and Y. Liu, 'Compact UWB-MIMO Antenna With High Isolation and Triple Band-Notched Characteristics', *IEEE Access*, vol. 7, pp. 19856–19865, 2019, doi: 10.1109/ACCESS.2019.2897170.
  32. M. S. Sharawi, 'Printed Multi-Band MIMO Antenna Systems and Their Performance Metrics [Wireless Corner]', *IEEE Antennas Propag Mag*, vol. 55, no. 5, pp. 218–232, Oct. 2013, doi: 10.1109/MAP.2013.6735522.
  33. M. S. Sharawi, M. A. Jan, and D. N. Aloji, 'Four-shaped 2×2 multi-standard compact multiple-input-multiple-output antenna system for long-term evolution mobile handsets', *IET Microwaves, Antennas & Propagation*, vol.

- 6, no. 6, pp. 685–696, 2012, doi: 10.1049/iet-map.2011.0528.
34. R. Karimian, H. Oraizi, S. Fakhte, and M. Farahani, 'Novel F-Shaped Quad-Band Printed Slot Antenna for WLAN and WiMAX MIMO Systems', *IEEE Antennas Wirel Propag Lett*, vol. 12, pp. 405–408, 2013, doi: 10.1109/LAWP.2013.2252140.
35. A. G. Alhaddad, R. A. Abd-Alhameed, D. Zhou, C. H. See, P. S. Excell, and S. M. R. Jones, 'Folded Loop Balanced Coplanar Antenna for WLAN Applications', *IEEE Trans Antennas Propag*, vol. 60, no. 10, pp. 4916–4920, Oct. 2012, doi: 10.1109/TAP.2012.2207322.
36. Constantine A. Balanis, *Antenna Theory: Analysis and Design*, 4th Edition. New Jersey: Wiley, 2016.
37. S. Ullah *et al.*, 'A Compact Frequency and Radiation Reconfigurable Antenna for 5G and Multistandard Sub-6 GHz Wireless Applications', *Wirel Commun Mob Comput*, vol. 2022, 2022, doi: 10.1155/2022/4658082.
38. Z. Zhang, Y. C. Jiao, Y. Song, T. L. Zhang, S. M. Ning, and F. S. Zhang, 'A modified CPW-fed monopole antenna with very small ground for multiband WLAN applications', *Microw Opt Technol Lett*, vol. 52, no. 2, pp. 463–466, Feb. 2010, doi: 10.1002/mop.24940.
39. S. P. Wadkar, B. G. Hogade, S. M. Rathod, H. Kumar, and G. Kumar, 'Normal Mode Helical Antenna on Small Circular Ground Plane', *IETE J Res*, vol. 66, no. 5, pp. 617–624, Sep. 2020, doi: 10.1080/03772063.2018.1510748.
40. M. Sanad, 'Microstrip antennas on very small ground planes for portable communication systems', in *Proceedings of IEEE Antennas and Propagation Society International Symposium and URSI National Radio Science Meeting*, IEEE, pp. 810–813. doi: 10.1109/APS.1994.407968.
41. Computer Simulation Technologies AG, 'CST Microwave Studio'. 2019.
42. L. Yang, T. Li, and S. Yan, 'Highly Compact MIMO Antenna System for LTE/ISM Applications', *Int J Antennas Propag*, vol. 2015, pp. 1–10, 2015, doi: 10.1155/2015/714817.
43. L. Malviya, R. K. Panigrahi, and M. V. Kartikeyan, 'Four Element Planar MIMO Antenna Design for Long-Term Evolution Operation', *IETE J Res*, vol. 64, no. 3, pp. 367–373, May 2018, doi: 10.1080/03772063.2017.1355755.



**Widad Faraj A. Mshwat** was born in Tripoli, Libya. She received a B.Sc. degree in electrical and electronic engineering from Tripoli University, Tripoli, in 1996, and an M.Sc. degree in communication and computer engineering from University Kebangsaan Malaysia, in 2004. She completed her Ph.D. degree in 2022 in wireless and mobile communications systems with the Faculty of Engineering and Informatics, University of Bradford. She was a Lecturer Assistant for one year at Tripoli University. She was the Head of the Training Section, at Almadar Telecom Company, for two years. She was appointed as a Lecturer, and the Head of the Communications Engineering Department, at Yafren Higher Institute, from 2004 to 2009. She was the Head of the Communications Department at the Higher Institute for Girls/Tripoli, from 2012 to 2015. She has

published and contributed to more than 20 journal and conference articles in the fields of wireless and mobile communications. Her research interests include simulation, design, and implementation of front-end antenna systems for millimeter-wave communications, multi-band/UWB antennas, MIMO systems, smartphone antennas, SAR/user-impact, full-duplex diversity antennas, 5G antennas, implementable/biomedical sensors, millimeter-wave/terahertz components, fractal structures, metamaterials and metasurfaces, EBG/FSS-inspired radiators, and reconfigurable antenna structures.



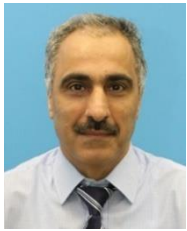
**Jamal Sulieman Kosha** was born in Tripoli, Libya. He received a B.Sc. degree in electronics and computer engineering from Tripoli University, Tripoli, in 1994, an M.Sc. degree in communication and computer engineering from University Kebangsaan Malaysia, in 2004, and an M.Sc. degree in human resources management from the University of Salford, in 2017, and the Ph.D. degree from the Radio Frequency and Sensor Design Research Group, University of Bradford, U.K., in 2022. He was a Lecturer Assistant for one year at Tripoli University. He was the Head of the Statistics & Information Office, at Almadar Telecom Company, for two years. He was appointed as a Lecturer, the Head of the IT Department, and the Deputy Director of the Yafren Higher Institute, from 2004 to 2009. He was an Active Member of the National Digital Trunking Network Team, in Libya, from 2005 to 2007. He was appointed as the Head of the Corporate Development Office, at Almadar Aljadid Telecom Company, from 2012 to 2018. He was able to publish and contribute over 15 journal and conference articles in the field of wireless and mobile communications. His research interests include simulation, design, and implementation of front-end antenna systems for millimeter-wave communications, multi-band/UWB antennas, MIMO systems, smartphone antennas, SAR/user-impact, 5G antennas, millimeter-wave/terahertz components, fractal structures, EBG/FSS-inspired radiators, and reconfigurable structures.



**Engr Abubakar Salisu**, is a member of the Nigerian Society of Engineers, The Council for the Regulation of Engineering in Nigeria, and the International Association of Engineers. He's currently a Ph.D. student at the Faculty of Engineering and Informatics, University of Bradford United Kingdom. He obtained his first degree in Electrical and Electronics Engineering from Abubakar Tafawa University Bauchi, Nigeria, and proceeded to pursue his master's degree in Electronics and Telecommunications Engineering at Universiti Teknologi Malaysia UTM, Malaysia. His areas of research include Antenna Design; Microstrip Antenna, Reconfigurable Antenna, MIMO Systems etc. He is also interested in Digital Communications and Antenna Optimization Using Artificial Intelligence. He is currently a Lecturer at the Department of Electrical and Electronics Engineering, Modibbo Adama University Yola, Adamawa State, Nigeria.



**Atta Ullah** was born in Mardan, Khyber Pakhtunkhwa, Pakistan. He received the B.Sc. and M.Sc. degrees in electronics engineering from the University of Peshawar, Pakistan, respectively, an M.Sc. degree in communication engineering from the University of York, U.K., in 2008, and a Ph.D. degree from the Radio Frequency and Sensor Design Research Group, University of Bradford, U.K., in 2022. He was a Research Fellow in the SATNEX V Project, funded by the European Space Agency. His research interests include simulation, design, and implementation of front-end antenna systems for millimeter-wave communications, multi-band/UWB antennas, phased arrays, MIMO systems, smartphone antennas, SAR/user-impact, full-duplex diversity antennas, 5G antennas, implementable/biomedical sensors, RFID tag antennas, millimeter-wave/terahertz components, fractal structures, metamaterials and metasurfaces, Fabry resonators, EBG/FSS-inspired radiators, band-pass/band-stop microwave filters, and reconfigurable structures.



**Nazar T Ali** (M'01SM'03) received the PhD degree in electrical and electronic engineering from the University of Bradford, UK, in 1990. From 1990 to 2000, he held various posts at the University of Bradford as a researcher and lecturer. He worked in many collaborative research projects in the UK under the umbrella of the centre of Research Excellence, Department of Trade and Industry (DTI), and EPSERC. This involved a consortium of a number of universities and industrial companies.

He is currently an associate professor at Khalifa University in the United Arab Emirates. His current research interests include antennas and RF circuits and systems, indoor and outdoor localization techniques, and RF measurements. He has over 100 articles published in peer reviewed high quality journals and conferences.



**Issa Elfargani** (Senior Member, IEEE) received the M.Sc. and Ph.D. degrees in electrical and electronic engineering from the University of Bradford, Bradford, U.K., in 2008 and 2013, respectively. In 2013, he was working as a Postdoctoral Researcher and then as an Investigator Junior at the Mobile Systems Group, Instituto de Telecomunicações, Universidade de Santiago, Aveiro, Portugal. He has several years of experience in 3G/4G and 5G radio frequency systems research with expertise on

several and different antenna structures along with novel approaches in accomplishing a size reduction, low cost, improved bandwidth, gain, and efficiency.



**Chan Hwang See** (Senior Member, IEEE) received the B.Eng. (Hons.) degree in electronic, telecommunication, and computer engineering and a Ph.D. degree from the University of Bradford, U.K., in 2002 and 2007, respectively. He is a Professor with the School of Computing, Engineering and the Built Environment, Edinburgh Napier University, U.K., where he was the Head of Electrical Engineering and Mathematics from 2019 to 2022. He is a coauthor for

one book and three book chapters. His research interests cover wireless sensor network system design, computational bioelectromagnetics, antennas, microwave circuits, Internet of Things (IoTs), microwave sensors, Wireless Power Transfer, and acoustic sensor design. He has published over 300 peer-reviewed journal articles and conference papers in these research areas. Since 2023, he has served as the UK representative for Commission K: Electromagnetics in Biology and Medicine within International Union of Radio Science (URSI). He was a recipient of two Young Scientist Awards from the International Union of Radio Science (URSI) and Asia-Pacific Radio Science Conference (AP-RASC) in 2008 and 2010, respectively. He was awarded a certificate of excellence for his successful Knowledge Transfer Partnership (KTP) with Yorkshire Water on the design and implementation of a wireless sensor system for sewerage infrastructure monitoring in 2009. He was awarded an IEEE Malaysia AP/MTT/EMC Joint Chapter Best Paper Award in 2020. He is a Chartered Engineer, and Fellow of the Institution of Engineering and Technology. He is also a Fellow of the Higher Education Academy, a full member of the EPSRC Review College, an Associate Editor for IEEE Access, and an Editor for Journal of Electronics and Electrical Engineering, Scientific Reports, PeerJ Computer Science, and Wireless Power Transfer Journals. According to Web of Science, he has completed over 500 verified reviews and over 250 verified editor records.



**Chemseddine Zebir** received a Ph.D. degree in electronics from the University of Constantine, Algeria, in 2011. He has been with the Department of Electronics, University of Ferhat Abbas, Setif, Algeria, since 2006, where he is currently an Associate Professor. He started working on reflector and microstrip antennas using moment method in time and spectral domains. He has published up to 90 journals and refereed conference articles. He is the author of four book chapters. His current research

interests include dielectric resonator antennas, MIMO antennas, mmWave

antennas, magnetic materials, and complex material components in microwave and optical domains.



**Jonathan Rodriguez** (Senior Member, IEEE) received the Ph.D. degree from the University of Surrey, U.K., in 2004. In 2005, he became a Researcher with Instituto de Telecomunicações, Portugal, and a Senior Researcher in 2008. Since 2017, he has been a Full Professor in mobile communications with The University of South Wales, U.K. He has served as a Project Coordinator for major international research projects (Eureka LOOP, FP7 C2POWER, and H2020-MSCA-SECRET), whilst acting as the Technical Manager for FP7 COGEU and FP7 SALUS. He is currently the Project Director of the PHYSEC Project funded under the NATO Science for PEACE and Security Program. He is the author of more than 600 published works on mobile communications and also serving as an Associate Editor for IEEE Access and IET Communications journal. His professional affiliations include C.Eng. (2013), FIET (2015), and FRSA (2022).



**Raed Abd-Alhameed** (M'02, SM'13) is currently a Professor of electromagnetic and radiofrequency engineering at the University of Bradford, U.K. He is also the Leader of radiofrequency, propagation, sensor design, and signal processing; in addition to leading the Communications Research Group for years within the School of Engineering and Informatics, University of Bradford. He has long years' research experience in the areas of radio frequency, signal processing, propagations, antennas, and electromagnetic computational techniques. He has published over 800 academic journals and conference papers; in addition, he has co-authored seven books and several book chapters including seven patents. He is a principal investigator for several funded applications to EPSRCs, Innovate UK, and the leader of several successful knowledge Transfer Programmes, such as with Arris (previously known as Pace plc), Yorkshire Water plc, Harvard Engineering plc, IETG Ltd., Seven Technologies Group, Emkay Ltd., and Two World Ltd. He has also been a co-investigator in several funded research projects including 1) H2020-MSCA-RISE-2024-2028; Marie Skłodowska-Curie, Research and Innovation Staff Exchange (RISE), titled: 6G Terahertz Communications for Future Heterogeneous Wireless Network, 2) HORIZON-MSCA-2021-SE-01-01, Type of Action: HORIZON-TMA-MSCA-SE -2027: ROBUST: Proposal title: "Ubiquitous eHealth Solution for Fracture Orthopaedic Rehabilitation" 3) Horizon 2020 research and innovation programme under grant agreement H2020-MSCA-RISE-2019-eBORDER-872878; 4) H2020 MARIE Skłodowska-Curie: Innovative Training Networks Secure Network Coding for Next Generation Mobile Small Cells 5G-US; 5) European Space Agency: Satellite Network of Experts V, Work Item 2.6: Frequency selectivity in phase-only beamformed user terminal direct radiating arrays; 6) Nonlinear and demodulation mechanisms in biological tissue (Dept. of Health, Mobile Telecommunications & Health Research Programme; and 7) Assessment of the Potential Direct Effects of Cellular Phones on the Nervous System (EU: collaboration with six other major research organizations across Europe). He was a recipient of the Business Innovation Award for his successful KTP with Pace and Datong companies on the design and implementation of MIMO sensor systems and antenna array design for service localizations. He is the chair of several successful workshops on energy-efficient and reconfigurable transceivers: Approach toward Energy Conservation and CO<sub>2</sub> Reduction that addresses the biggest challenges for future wireless systems. He is also the general chair of the IMDC-IST International Conference since 2020. He is a co-editor for Electronics MDPI Journal since June 2019; in addition, he was a Guest Editor of IET Science, Measurements and Technology Journal since 2009. He has been a Research Visitor of Wrexham University, Wales, since 2009, covering the wireless and communications research areas. His interest in computational methods and optimizations, wireless and mobile communications, sensor design, EMC, beam steering antennas, energy-efficient PAs, and RF predistorter design applications. He is a fellow of the Institution of Engineering and Technology a fellow of the Higher Education Academy and a Chartered Engineer.